Acta Crystallographica Section F
Structural Biology Communications
ISSN 2053-230X

Crystallization and preliminary X-ray study of TsiV3 from *Vibrio cholerae*

Jiulong Zhang,[a] Heng Zhang,[b] Ying Liu,[c] Lihong Zhan,[a] Zhun She,[c] Cheng Dong[c,d]* and Yuhui Dong[c]*

[a]School of Life Sciences, University of Science and Technology of China, 96 Jinzhai Road, Hefei, Anhui 230026, People's Republic of China, [b]State Key Laboratory of Protein and Plant Gene Research, School of Life Sciences, Peking University, No. 5 Yiheyuan Road, Beijing 100871, People's Republic of China, [c]Beijing Synchrotron Radiation Facility, Institute of High Energy Physics, Chinese Academy of Sciences, Beijing 100049, People's Republic of China, and [d]State Key Laboratory of Medicinal Chemical Biology, Nankai University, Tianjin 300071, People's Republic of China

Correspondence
e-mail: dongcheng@ihep.ac.cn, dongyh@ihep.ac.cn

Received 20 November 2013
Accepted 22 January 2014

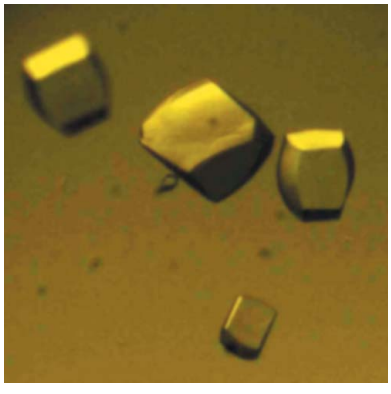

The bacterial type VI secretion system (T6SS), a dynamic organelle, participates in microbial competition by transporting toxic effector molecules to neighbouring cells to kill competitors. TsiV3, a recently defined T6SS immunity protein in *Vibrio cholerae*, possesses self-protection against killing by T6SS predatory cells by directly binding to and inhibiting their effector protein VgrG-3. Structural information about TsiV3 could help to illuminate its specific mechanism. In this study, TsiV3 from *V. cholerae* was cloned, expressed and crystallized and single-crystal X-ray diffraction data sets were collected to a resolution of 2.55 Å. Specifically, the crystal belonged to space group $P2_12_12_1$, with unit-cell parameters a = 73.3, b = 78.12, c = 106.18 Å. Matthews coefficient calculations indicated that the crystal may contain six TsiV3 molecules in one asymmetric unit, with a V_M value of 2.25 Å^3 Da^{-1} and a solvent content of 45.42%.

1. Introduction

The recently discovered bacterial type VI secretion system (T6SS) is present in *Vibrio cholerae*, which can cause diarrhoeal diseases such as cholera and mild gastroenteritis (Pukatzki *et al.*, 2006). T6SS allows *V. cholerae* to kill target cells through the translocation of toxic effector molecules in a cell–cell contact-dependent antagonistic way during various competition scenarios (Russell *et al.*, 2011). A typical T6SS gene cluster generally contains 15–25 genes and is highly conserved (Basler *et al.*, 2012). Surprisingly, both the conserved **h**aemolysin **c**oregulated **p**rotein (Hcp) that forms a membrane-spanning nanotube with an internal diameter of 4 nm (Ballister *et al.*, 2008) and **v**aline–**g**lycine **r**epeat **G** (VgrG) proteins (VgrG-1–VgrG-3) are secreted in the products of these T6SS genes and are required for the function of the T6SS machine; they represent two hallmark proteins of T6SS (Pukatzki *et al.*, 2007, 2009). Bioinformatic and structural analyses have suggested that VgrG-related proteins can assemble into a trimeric complex that is a structural homologue of the bacteriophage T4 needle or spike complex (Leiman *et al.*, 2009; Pukatzki *et al.*, 2007). This trimeric VgrG complex is located at the tip of the transmembrane nanotube comprised of hexameric rings formed by Hcp (Ballister *et al.*, 2008), and it can pierce the adjacent cell using its spike-shaped carboxy-terminal β-helical domain to kill prey cells (Shneider *et al.*, 2013). VgrG proteins possess additional C-terminal domains that act as effectors to attack prey cells, as found in VgrG-1 and VgrG-3 of the three VgrG proteins (VgrG-1, VgrG-2 and VgrG-3) encoded by the T6SS genes of *V. cholerae* (Pukatzki *et al.*, 2007). Previous studies have shown that VgrG-3 from *V. cholerae* contains a peptidoglycan-binding domain (PG1) at the C-terminus (Pukatzki *et al.*, 2009) and that this domain plays an important role in hydrolyzing the cell wall of Gram-negative bacteria, thereby granting *V. cholerae* a competitive advantage against adjacent cells (Brooks *et al.*, 2013).

Recently, the TsiV3 gene from *V. cholerae* that encodes a novel immunity protein required for self-protection to avoid T6SS-mediated self-intoxication was identified and the upstream gene product of TsiV3, VgrG-3, was identified as its corresponding effector protein (Dong, Ho *et al.*, 2013). Subsequently, it was reported that

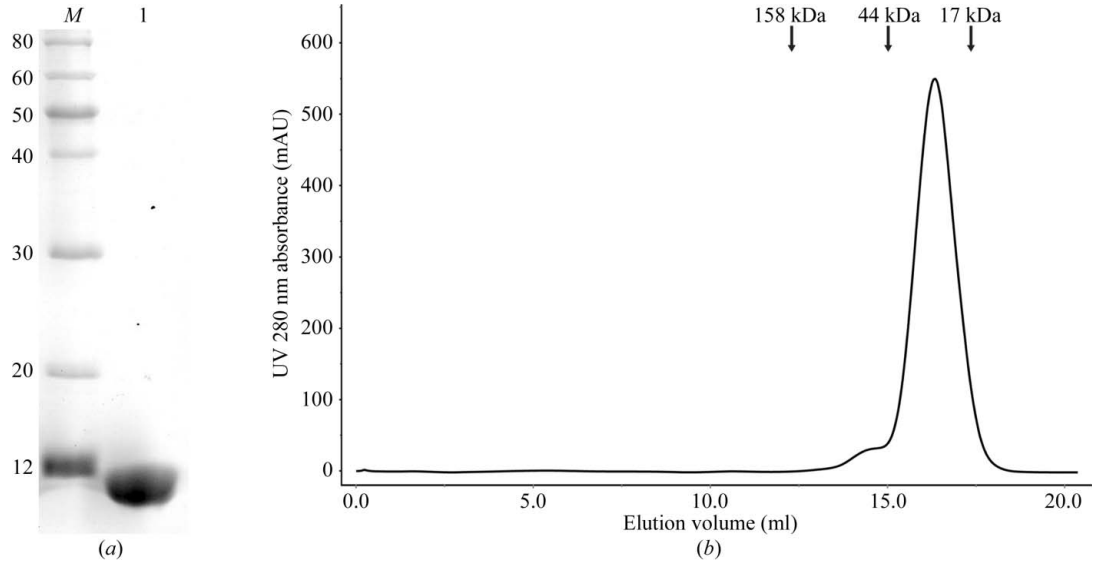

Figure 1
(*a*) 15% SDS–PAGE analysis of TsiV3. Lane *M*, molecular-mass standards (labelled in kDa); lane 1, purified TsiV3 protein (11 kDa). (*b*) Size-exclusion chromatography of TsiV3. The elution volume of TsiV3 is 16.3 ml, which is consistent with a homodimeric state.

TsiV3 (TsaB) directly binds to and inhibits effector protein VgrG-3 in a type II toxin–antitoxin (TA) manner and thus presents immunity to the toxic activity of VgrG-3 (Brooks *et al.*, 2013). As a novel T6SS immunity protein, TsiV3 does not share high sequence identity with other immunity proteins of known structure (Q9I2Q0, C6BHF3, Q8ZRL5, Q9HYC4, Q4KC91 and Q9I0D9; Shang *et al.*, 2012; Dong, Zhang *et al.*, 2013; Zhang *et al.*, 2013; Wang *et al.*, 2013; Whitney *et al.*, 2013; Li *et al.*, 2012). Moreover, little detail is known of how TsiV3 inhibits VgrG-3. However, it is believed that TsiV3 possesses the essential function of self-defence by resisting attack by other T6SSs. Structural characterization of TsiV3 may be the key to elucidating its inhibitory mechanism and may help in finding structural homologues to further classify immunity proteins. In an effort to determine the three-dimensional structure of TsiV3 by X-ray crystallography, this immunity protein TsiV3 was cloned, expressed, purified and crystallized. We obtained single crystals of TsiV3 in different conditions and report their preliminary crystallographic analyses.

2. Materials and methods

2.1. Cloning and expression

The coding sequence for TsiV3 (amino acids 25–122) was PCR-amplified from the genomic DNA of *V. cholerae* using the primers 5′-CATG**CCATGGGT**GAAAACTGCAATGATACATCTGG-3′ and 5′-CCG**CTCGAG**CAAACTATTATCAACATCCTCTA-3′; bold sequences represent *Nco*I and *Xho*I restriction sites, respectively. The product was cloned between the *Nco*I and *Xho*I restriction sites of the expression vector pET-28a (Novagen) with a hexahistidine tag at the C-terminus as described previously (Brooks *et al.*, 2013). After sequencing, the plasmid was transformed into *Escherichia coli* BL21 (DE3) competent cells (Novagen, USA). The cells were incubated at 310 K in 2.0 l LB medium containing 50 mg l^{-1} kanamycin. When the OD_{600} reached about 0.8, the cells were incubated at 289 K for 20 min, and 1 m*M* isopropyl *β*-D-1-thiogalactopyranoside (final concentration) was then added for induction at 289 K. Growth of the cells was continued at 289 K for 18 h. Finally, the cultured cells were harvested by centrifugation at 4500*g* for 30 min at 277 K.

2.2. Purification

The harvested cells were resuspended in 80 ml lysis buffer (20 m*M* Tris–HCl pH 8.0, 400 m*M* sodium chloride) and lysed by sonication on ice. The lysate was then centrifuged at 15 000*g* for 40 min at 277 K. Subsequent purification steps were all performed at 277 K. The supernatant was applied onto an Ni–NTA affinity column (GE Healthcare) pre-equilibrated with lysis buffer. The nonspecifically bound protein was removed by washing the column with 150 ml washing buffer (20 m*M* Tris–HCl pH 8.0, 150 m*M* sodium chloride, 40 m*M* imidazole). The affinity-bound protein was eluted with 40 ml elution buffer (20 m*M* Tris–HCl pH 8.0, 100 m*M* sodium chloride, 500 m*M* imidazole). Subsequently, the eluted protein was concentrated to 5 ml with a Millipore 10 kDa centrifugal device and purified by ion-exchange chromatography on a HiTrap Q FF column (GE Healthcare) pre-equilibrated with buffer *A* (20 m*M* Tris–HCl pH 8.0, 100 m*M* sodium chloride). The sample was eluted with a linear gradient from 0 to 45% buffer *B* (20 m*M* Tris–HCl pH 8.0, 1 *M* sodium chloride) over 12 min. The relevant fractions were concentrated by centrifugal ultrafiltration (Millipore, 10 kDa) to a volume of about 2 ml. The sample was further loaded onto a HiLoad 16/60 Superdex 200 (GE Healthcare) size-exclusion column previously equilibrated with 20 m*M* Tris–HCl pH 8.0, 150 m*M* sodium chloride. The relevant fractions were pooled and concentrated to 16 mg ml^{-1} using a Millipore 10 kDa centrifugal ultrafiltration device without changing the buffer. The purity of TsiV3 was analyzed by 12%(*w*/*v*) SDS–PAGE (Fig. 1*a*). The oligomerization state of TsiV3 from size-exclusion chromatography was estimated as a dimer (Fig. 1*b*).

2.3. Crystallization

The concentrated protein was centrifuged at 13 000*g* for 35 min at 277 K before use in crystallization trials. Initially, crystallization conditions of TsiV3 were screened by the sitting-drop vapour-diffusion method by mixing 1 µl protein solution and 1 µl reservoir solution and equilibrating against 100 µl reservoir solution using the Crystal Screen, Crystal Screen 2, Index, PEG/Ion, PEG/Ion 2, PEGRx and PEGRx 2 reagent kits (Hampton Research) at 277 and 293 K. Crystals appeared after 10 d in several conditions. The single

Table 1
Data-collection statistics for TsiV3.

Values in parentheses are for the highest resolution shell.

Source	Beamline 3W1A, BSRF
Space group	$P2_12_12_1$
Unit-cell parameters (Å)	a = 73.3, b = 78.12, c = 106.18
Wavelength (Å)	1.0000
Resolution range (Å)	50.00–2.55 (2.59–2.55)
Total/unique reflections	144769/20390
Completeness (%)	99.94 (99.9)
$R_{\rm merge}$† (%)	3.9 (39.9)
$\langle I/\sigma(I)\rangle$	31.7 (2.3)

† $R_{\rm merge} = \sum_{hkl}\sum_i |I_i(hkl) - \langle I(hkl)\rangle| / \sum_{hkl}\sum_i I_i(hkl)$, where $I_i(hkl)$ is the intensity of the ith measurement of reflection hkl and $\langle I(hkl)\rangle$ is the weighted average intensity for all observations i of reflection hkl.

crystals that were used for X-ray diffraction measurements were obtained at 277 K in a condition consisting of 0.2 *M* ammonium citrate tribasic pH 7.0, 20%(*w*/*v*) polyethylene glycol monomethyl ether 2000, 0.1 *M* imidazole pH 7.0.

2.4. Data collection and analysis

For data collection, the crystals were mounted in a nylon-fibre loop, transferred into solution corresponding to the reservoir solution supplemented with cryoprotectant solution [20%(*v*/*v*) glycerol] and flash-cooled in liquid nitrogen. X-ray diffraction data were collected using a MAR CCD detector (crystal-to-detector distance of 200 mm, 1° oscillation per image, total rotation angle of 180°) on beamline 3W1A of the Beijing Synchrotron Radiation Facility (BSRF), China. Subsequently, the data were processed using the *HKL*-2000 program package (Otwinowski & Minor, 1997). Detailed data-collection statistics are given in Table 1.

3. Results and discussion

TsiV3 was predicted to contain a 24-amino-acid signal peptide at its N-terminus by *Phobius* prediction (http://phobius.sbc.su.se). TsiV3 (amino acids 25–122) was cloned and subsequently expressed with a fused C-terminal hexahistidine tag in *E. coli* BL21 cells. Sufficient and highly pure TsiV3 protein could be obtained after purification by Ni–NTA chromatography. When this protein was further purified by ion-exchange chromatography on a HiTrap Q FF column connected to an ÄKTApurifier 100 system, two separated peaks appeared (data not shown). The collected protein from each peak was purified by size-exclusion chromatography. The result suggested that the TsiV3 protein in the first peak existed in a homodimeric state (Fig. 1*b*) and the TsiV3 protein in the second peak was highly oligomeric or aggregated (data not shown). Purified TsiV3 was observed upon SDS–PAGE analysis with an apparent molecular weight of 11.0 kDa (Fig. 1*a*).

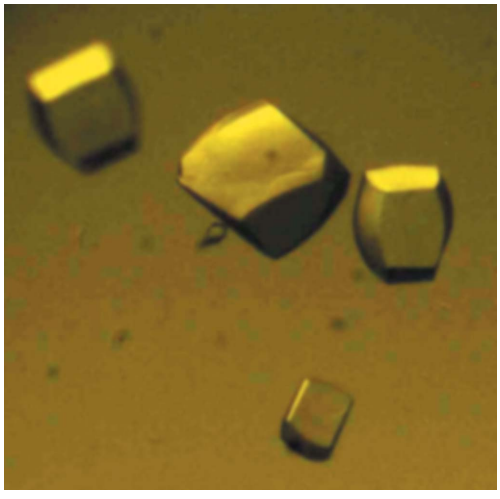

Figure 2
Crystals of TsiV3 grown under the condition 0.2 *M* ammonium citrate tribasic pH 7.0, 20%(*w*/*v*) polyethylene glycol monomethyl ether 2000, 0.1 *M* imidazole pH 7.0.

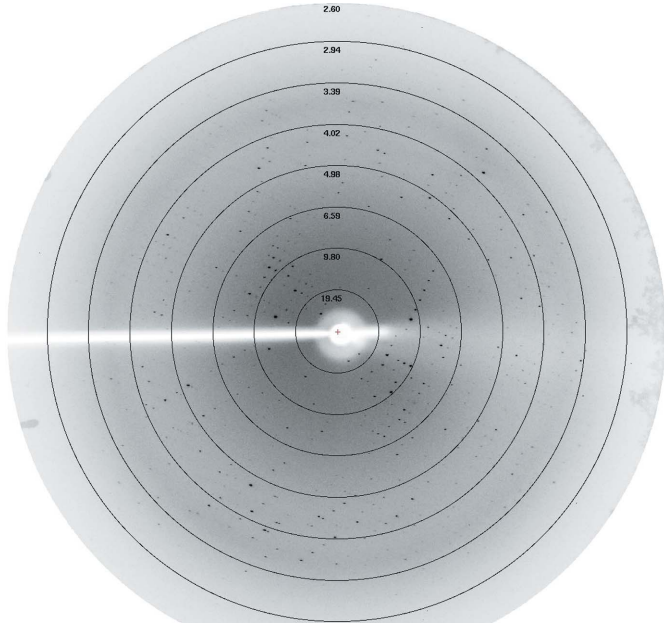

Figure 3
An X-ray diffraction image (labelled in Å) of the TsiV3 crystal obtained at the Beijing Synchrotron Radiation Facility (BSRF), China.

Crystals could be obtained in different conditions using the dimeric protein for screening (Fig. 2). We collected a complete diffraction data set (Fig. 3) from a single crystal which displayed a good-quality diffraction pattern. This crystal diffracted to 2.55 Å resolution and belonged to space group $P2_12_12_1$, with unit-cell parameters a = 73.3, b = 78.12, c = 106.18 Å. The data-collection statistics are reported in Table 1. The *CCP*4 suite (Winn *et al.*, 2011) was used to calculate the Matthews coefficient as 2.25 Å^3 Da^{-1} (Matthews, 1968). The asymmetric unit is most likely to contain six molecules, with a corresponding solvent content of 45.42%. The molecular-replacement phasing method (MR) was not used to attempt to solve the TsiV3 crystal structure owing to the lack of an appropriate search model. A selenomethionine-substituted protein for single-wavelength anomalous diffraction (SAD) phasing has now been prepared in an effort to determine the structure of TsiV3.

The authors thank Zengqiang Gao and Haidai Hu for helpful discussions and analyses. We would like to acknowledge the Beijing Synchrotron Radiation Facility (BSRF) for crystal diffraction data collection. This project was financially supported by grants from the National Basic Research Program of China (2012CB917203) and the National Natural Science Foundation of China (10979005).

References

Ballister, E. R., Lai, A. H., Zuckermann, R. N., Cheng, Y. & Mougous, J. D. (2008). *Proc. Natl Acad. Sci. USA*, **105**, 3733–3738.

Basler, M., Pilhofer, M., Henderson, G. P., Jensen, G. J. & Mekalanos, J. J. (2012). *Nature (London)*, **483**, 182–186.
Brooks, T. M., Unterweger, D., Bachmann, V., Kostiuk, B. & Pukatzki, S. (2013). *J. Biol. Chem.* **288**, 7618–7625.
Dong, C., Zhang, H., Gao, Z.-Q., Wang, W.-J., She, Z., Liu, G.-F., Shen, Y.-Q., Su, X.-D. & Dong, Y.-H. (2013). *Biochem. J.* **454**, 59–68.
Dong, T. G., Ho, B. T., Yoder-Himes, D. R. & Mekalanos, J. J. (2013). *Proc. Natl Acad. Sci. USA*, **110**, 2623–2628.
Leiman, P. G., Basler, M., Ramagopal, U. A., Bonanno, J. B., Sauder, J. M., Pukatzki, S., Burley, S. K., Almo, S. C. & Mekalanos, J. J. (2009). *Proc. Natl Acad. Sci. USA*, **106**, 4154–4159.
Li, M., Le Trong, I., Carl, M. A., Larson, E. T., Chou, S., De Leon, J. A., Dove, S. L., Stenkamp, R. E. & Mougous, J. D. (2012). *PLoS Pathog.* **8**, e1002613.
Matthews, B. W. (1968). *J. Mol. Biol.* **33**, 491–497.
Otwinowski, Z. & Minor, W. (1997). *Methods Enzymol.* **276**, 307–326.
Pukatzki, S., Ma, A. T., Revel, A. T., Sturtevant, D. & Mekalanos, J. J. (2007). *Proc. Natl Acad. Sci. USA*, **104**, 15508–15513.
Pukatzki, S., Ma, A. T., Sturtevant, D., Krastins, B., Sarracino, D., Nelson, W. C., Heidelberg, J. F. & Mekalanos, J. J. (2006). *Proc. Natl Acad. Sci. USA*, **103**, 1528–1533.
Pukatzki, S., McAuley, S. B. & Miyata, S. T. (2009). *Curr. Opin. Microbiol.* **12**, 11–17.
Russell, A. B., Hood, R. D., Bui, N. K., LeRoux, M., Vollmer, W. & Mougous, J. D. (2011). *Nature (London)*, **475**, 343–347.
Shang, G., Liu, X., Lu, D., Zhang, J., Li, N., Zhu, C., Liu, S., Yu, Q., Zhao, Y., Zhang, H., Hu, J., Cang, H., Xu, S. & Gu, L. (2012). *Biochem. J.* **448**, 201–211.
Shneider, M. M., Buth, S. A., Ho, B. T., Basler, M., Mekalanos, J. J. & Leiman, P. G. (2013). *Nature (London)*, **500**, 350–353.
Wang, T., Ding, J., Zhang, Y., Wang, D.-C. & Liu, W. (2013). *Acta Cryst.* D**69**, 1889–1900.
Whitney, J. C., Chou, S., Russell, A. B., Biboy, J., Gardiner, T. E., Ferrin, M. A., Brittnacher, M., Vollmer, W. & Mougous, J. D. (2013). *J. Biol. Chem.* **288**, 26616–26624.
Winn, M. D. *et al.* (2011). *Acta Cryst.* D**67**, 235–242.
Zhang, H., Zhang, H., Gao, Z.-Q., Wang, W.-J., Liu, G.-F., Xu, J.-H., Su, X.-D. & Dong, Y.-H. (2013). *J. Biol. Chem.* **288**, 5928–5939.